

# Two stages for visual object tracking

Fei Chen, *Student Member, IEEE*, Xiaodong Wang *Member, IEEE*

## Abstract

Siamese-based trackers have achieved promising performance on visual object tracking tasks. Most existing Siamese-based trackers contain two separate branches for tracking, including classification branch and bounding box regression branch. In addition, image segmentation provides an alternative way to obtain the more accurate target region. In this paper, we propose a novel tracker with two-stages: detection and segmentation. The detection stage is capable of locating the target by Siamese networks. Then more accurate tracking results are obtained by segmentation module given the coarse state estimation in the first stage. We conduct experiments on four benchmarks. Our approach achieves state-of-the-art results, with the EAO of 52.6% on VOT2016, 51.3% on VOT2018, and 39.0% on VOT2019 datasets, respectively.

## Index Terms

Siamese-based, visual object tracking, detection, segmentation

## I. INTRODUCTION

VISUAL object tracking is a challenging problem in computer vision. It aims to track a target at each frame over a video sequence, given only its location and size in the first frame. The tracking process is influenced by many challenging scenarios, such as appearance changes, occlusion, illumination, deformation, motion blur, viewpoint change, and fast moving so on. Recently, deep learning technologies have significantly promoted the task of visual object tracking, which obtained fast tracking speed and accurate tracking results, benefiting from the powerful deep features and bounding box regression technologies. While accurate target localization, scale and aspect ratio estimation are still the challenging problem in the field of visual object tracking. In recent years, cross-correlation play an important role which converts the spatial correlation operation into Fourier domain to speeds up the detection process [1]. Afterwards, CFNet[2] firstly integrated the correlation into the convolutional neural networks as a layer and can be trained in an end-to-end way. Recently, the Siamese-based tracker like SiamRPN [3] equip the Siamese backbone networks with the Region Proposal Networks (RPN) to obtain accurate bounding boxes, which can be trained end-to-end in offline phase. To enhance the discriminative ability, Ocean [4] adds an global object aware module after the conventional local classifier module within the anchor-free framework. The object aware module aligns the features with the predicted region for each location, which enhance the ability of classifier to distinguish the target and background. In addition to bounding box regression in most existing deep trackers, segmentation based visual trackers [5], [6] introduce the segmentation network to obtain the rotated bounding boxes, aiming to match well with the datasets like VOT-2016 [7], VOT-2018 [8], and VOT-2019 [9]. While the limitation in SiamMask [5] is that the segmentation branch coupled with classification branch and bounding box regression branch lead to the difficulty to train the whole networks. Although applying the deep convolutional neural network (i.g., ResNet50) as backbone to extract features, the robustness still has much room need to be improved, even compared with the correlation filters based trackers [10], [11]. In this paper, to address the above limitations, we proposed a two stage tracker that embrace both the Siamese network and segmentation. Firstly, the outputs of Siamese network provide the coarse localization and scale and ratio estimation of the target. Then, the segmentation network is designed to predict the segmentation mask between target and background. Finally, the rotated bounding box is fitted to the predicted mask. Our two stage tracking-by-segmentation approach outperforms most of the state-of-the-art trackers on the popular benchmarks [7], [8], [9].

## II. RELATED WORK

In this section, we review the related work on visual object tracking.

**correlation filter based trackers.** In the last few years, correlation filters based trackers have significantly promoted the tracking performance when it was first proposed by Bolme et al. [1]. Danelljan et al. [12] adds the spatial regularization in the learning process to penalize correlation filters coefficients depending on their spatial location. Li et al. [10] introduce both the spatial and temporal regularizations into the learning. In ASRCF [13], the spatial regularization weight is also learned adaptively like the correlation filter during tracking. To embrace the power of deep features, Valmadre et al. [2] implemented the correlation filter as a layer in a Siamese network and performed tracking by cross-correlation between the template filter and search image.

**Siamese networks based trackers.** Recently, Siamese networks based trackers have attracted great attention and achieved promising performance due to their end-to-end training capabilities and high efficiency during tracking. Bertinetto et al. [14]

Fei Chen is with the College of Computer, National University of Defense Technology, Changsha 410073, China(e-mail: chenfei14@nudt.edu.cn).

Xiaodong Wang is with the College of Computer, National University of Defense Technology, Changsha 410073, China(e-mail: xdwang@nudt.edu.cn).

introduced fully convolutional Siamese networks to extract feature maps of exemplar and search images. And the simple cross-correlation layer enables the tracker operates at beyond real-time tracking speed. To obtain more accurate bounding boxes, SiamRPN [3] utilized the Region Proposal Networks to generate prior defined anchors. DaSiamRPN [15] improved the discriminative ability by the collected hard negative samples in offline training and a distractor-aware module was introduced in tracking which aims to continuously discover hard negative samples (distractors) used for online learning the templates. Afterwards, SiamRPN++ further took the advantages of deeper networks such as ResNet-50 as their backbone and proposed a depth-wise cross-correlation layer produce the similarity maps for classification and bounding box regression.

**Segmentation based trackers.** Another kind of trackers are that both predict bounding boxes as well as the class-agnostic binary segmentation. In SiamMask [5], Wang et al. proposed an end-to-end framework for producing bounding boxes and the class-agnostic object segmentation masks [16] at the same time. The whole network includes classification branch, box generation branch, and segmentation branch, which can be trained together in offline phase. In D3S [6], they proposed a single-shot discriminative segmentation tracker, which combined geometrically invariant model (GIM) and geometrically constrained Euclidean model (GEM). The geometrically invariant model takes the target and background deep feature vectors as inputs to produce foreground and background similarity. While the GEM applies the DCF to generate confidence map of target presence. We found that the performance of the tracking depends heavily on the target localization by the GEM model.

### III. REVISITING THE SIAMRPN++

Siamese networks based trackers have shown their promising performance in visual object tracking. SiamRPN++ introduced a depthwise cross-correlation layer in their RPN module which requires fewer parameters than up-channel cross-correlation in SiamRPN [3]. The template patch  $z$  is usually given by the bounding box in the first frame of the sequence. For a following frame  $x$  in the sequence, the goal of SiamRPN++ is to find the best match between the target patch  $z$  and search patch  $x$  by cross-correlation as:

$$P = \phi(z) \star \phi(x) \quad (1)$$

where  $\phi(z)$  and  $\phi(x)$  are the output feature maps of Siamese subnetworks. The template branch and search branch share parameters in feature extraction subnetwork except region proposal subnetwork. SiamRPN++ reduce the influence of center bias by the spatial aware sampling strategy in offline training. In addition, multi-layer aggregation strategy is adopted to enhance the discriminative ability of tracker. In order to equip deep network like ResNet-50 into the tracking framework, the large stride of 32 pixels in original ResNet-50 has been decreased to 8 pixels to increase the resolution of feature maps of high layers.

### IV. OUR APPROACH

In this paper, we propose an two-stage tracking framework to fully take advantages of bounding boxes regression of Siamese network and the class-agnostic segmentation module of D3S. As shown in Fig.1, our approach consists of a backbone network, a detection module, and a segmentation model. The backbone network is utilized for extract feature maps of the template patch and search patch. The detection module contains two branches that include classification branch and bounding box regression branch. The classification branch is utilized to perform foreground-background classification, and the regression branch aims to estimate the bounding box on each of the location.

In this paper, to reduce computation and adapt to shape variations, we apply an anchor-free detector for target localization. For a feature map  $f_i \in R^{H \times W}$ , we have  $H \times W$  candidate locations for target object. For a ground-truth bounding box  $B^i = \{x_0, y_0, x_1, y_1\}$ , where  $(x_0, y_0)$ ,  $(x_1, y_1)$  denote the top-left and bottom-right points of it, respectively. Let  $(x, y)$  denotes a location in  $f_i$ , it is considered as a positive sample if it falls into any ground-truth bounding boxes  $B^i$ . The regression target is a 4D real vector  $T = \{t^*, l^*, b^*, r^*\}$ , where  $t^*$ ,  $l^*$ ,  $b^*$ , and  $r^*$  are the distance from four sides (i.g., top, left, bottom, and right) of the bounding box to the target center  $(x, y)$ . Then the training targets for the location  $(x, y)$  can be computed as:

$$l^* = x - x_0, r^* = x_1 - x, t^* = y - y_0, b^* = y_1 - y \quad (2)$$

At the inference stage, for a location  $(c_x, c_y)$ , the predicted bounding box can be computed by:

$$x_0 = c_x - l_p^*, y_0 = c_y - t_p^*, x_1 = c_x + r_p^*, x_2 = c_y + b_p^* \quad (3)$$

where  $l_p^*$ ,  $t_p^*$ ,  $r_p^*$ , and  $b_p^*$  are the outputs of bounding box regression branch. Then the final target state is obtained by selecting the position with highest confidence score and the corresponding bounding box.

When the state of the target was available in the detection stage, we then activate the segmentation module which takes the template patch, search patch, and detected bounding box as inputs. As the Figure.2 shows. We borrow the main framework from D3S [6], while we utilized the ConvTransposed2D module to upsample the feature maps from high layer to be the same with low layer. For a upsampling layer, the feature maps from the backbone are added to enrich its information. The final upscaling module if followed by a softmax to produce the segmentation probability map. Then we binarise the output of probability map with a threshold 0.5 to produce the final mask.

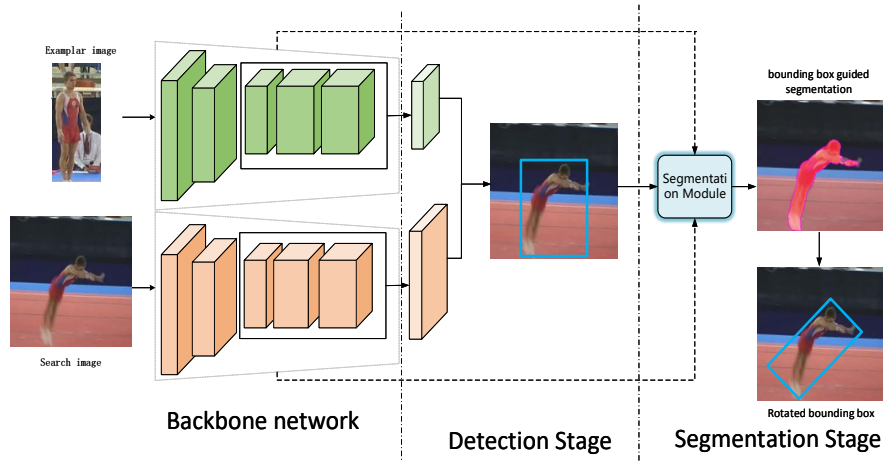


Fig. 1. An overview of our tracking approach. The backbone network is utilized to extract feature representations for exemplar patch and search patch. Then the classification branch and regression branch in the detection module predict the bounding box of target object. Finally, the target state and deep features from backbone network are fed into segmentation module to estimate the accurate rotated bounding box.

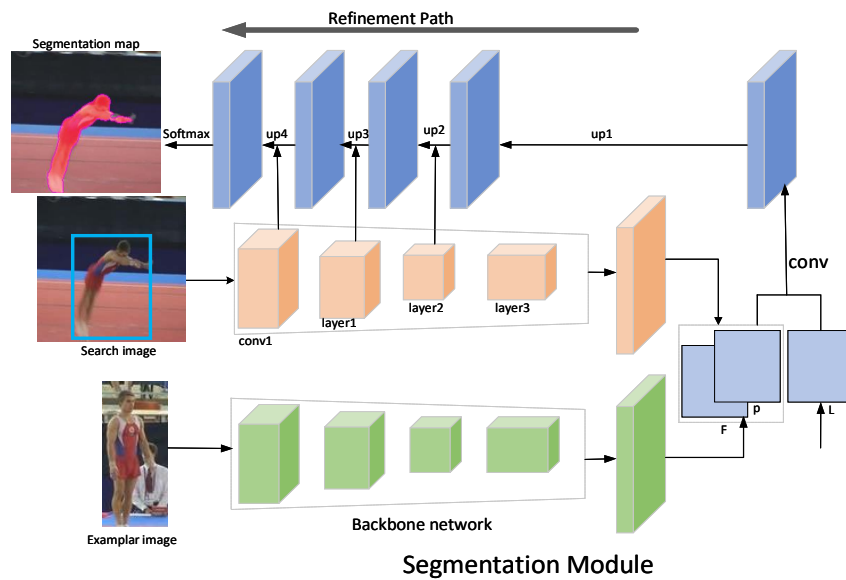


Fig. 2. The segmentation module in our tracker. In the refinement module, feature maps of conv1, layer1, and layer2 from ResNet-50 are added to last three sampling modules, respectively.

## V. EXPERIMENTS

We perform a comprehensive analysis of our approach on four challenging datasets, including VOT-2016 [7], VOT-2018 [8], VOT-2019 [9], GOT-10k [17], and LaSOT [18] datasets. The performance in VOT datasets is evaluated in terms of accuracy and robustness. The accuracy measures the average overlap among the successfully tracked frames and the robustness measures how many times the tracker loses the target during tracking. The failure indicates that the overlap between the predicted bounding box and the ground truth becomes zero. The EAO takes both the accuracy and robustness into account, which aims to address the problem of increased variance and bias of AverageOverlap (AO) measure due to variable sequence lengths.

### A. Implementation details

For the detector in first stage, we apply the online tracker of Ocean [4] as our baseline. The ResNet-50 is utilized as the backbone for both of the detector and segmentation modules. The segmentation networks are pre-trained on the Youtube-VOS [19] dataset. Our approach is implemented using Python 3.7 and PyTorch 1.1.0 with Intel(R) i5-7500 3.4 GHz CPU, 64 RAM, and Nvidia GTX 1080Ti.

## B. State-of-the-art comparison

In this section, we compare our approach with several state-of-the-art trackers on four tracking benchmarks.

**VOT-2016 [7]:** This dataset contains 60 sequences from VOT2015 with more accurate ground-truth bounding boxes, where each sequence is per-frame annotated by five attributes: occlusion, illumination change, motion change, size change, and camera motion. As shown in Table.I, we compare our approach with several outstanding trackers include ECO [20], SiamRPN++ [21], SiamBAN [22], DaSiamRPN [15], D3S [6], ATOM [23], and DiMP [24]. Compare with D3S, our approach achieves similar accuracy, but obtains a significant gain of 3.3% over D3S in terms of EAO and accuracy increases by 0.05%. Among these trackers, our tracker has both the highest EAO and accuracy.

TABLE I

COMPARISON RESULTS ON VOT2016 DATASET WITH PERFORMANCE MEASURES OF EAO, ACCURACY, AND ROBUSTNESS, WHERE A DENOTES THE ACCURACY AND RO DENOTES THE ROBUSTNESS.

	ECO	ATOM	DiMP	SiamRPN++	DaSiamRPN	SiamBAN	D3S	Ours
EAO↑	0.374	0.424	0.479	0.478	0.401	0.505	0.493	0.526
A ↑	0.54	0.617	0.624	0.637	0.609	0.632	0.66	0.671
Ro ↓	0.2	0.189	0.135	0.177	0.224	0.149	0.131	0.131

**VOT-2018 [8]:** All sequences in VOT-2018 maintains the same sequences with VOT2016, where the least challenging sequences in VOT2016 are replaced by new sequences. As shown in Table. II, our tracker achieves the EAO of 51.3% and accuracy of 66.2 %, respectively. Our approach achieves a gain of 2.4 % over D3S and OceanOn. Our tracker ranks second in terms of robustness.

TABLE II

COMPARISON RESULTS ON VOT2018 DATASET WITH PERFORMANCE MEASURES OF EAO, ACCURACY, AND ROBUSTNESS.

	ATOM	DiMP	SiamRPN++	DaSiamRPN	SiamBAN	D3S	OceanOn	Ours
EAO↑	0.401	0.44	0.415	0.326	0.447	0.489	0.489	0.513
A ↑	0.59	0.597	0.6	0.57	0.59	0.64	0.592	0.662
Ro ↓	0.201	0.152	0.234	0.337	0.178	0.15	0.117	0.15

**VOT-2019 [9]:** In this dataset, 12 new sequences selected from the update pool of 1000 sequences collected from GOT-10k dataset. And the 12 least difficult sequences of VOT2018 are replaced by the new selected sequences. Meanwhile, the segmentation masks were manually created for tracking targets in all frames of the new sequences, and the rotated bounding boxes for tracking targes are also provided. Compared with previous datasets, VOT-2019 poses new challeng for trackers. Our tracker achieves a gain of 4.2% and 4 % over D3S and OceanOn in terms of EAO, respectively. Compared to D3S, the accuracy increases to 65.8 % and the failure rates deceases to 27.6%. This illustrates that our tracker can obtain more accurate bounding boxes with good robustness.

TABLE III

COMPARISON RESULTS ON VOT2019 DATASET WITH PERFORMANCE MEASURES OF EAO, ACCURACY, AND ROBUSTNESS.

	SiamMASK	ATOM	DiMP	SiamRPN++	SiamBAN	D3S	OceanOn	Ours
EAO↑	0.287	0.301	0.379	0.292	0.322	0.348	0.350	0.390
A ↑	0.594	0.603	0.594	0.580	0.596	0.646	0.594	0.658
Ro ↓	0.461	0.411	0.278	0.446	0.396	0.331	0.316	0.276

**GOT-10k [17]:** This is a large-scale tracking dataset which contains 10,000 sequences in training set and 180 sequences in testing set. There is no overlap between the training set and testing set. GOT-10k uses average overlap (AO) and success rate (SR) to evaluate the trackers. AO denotes the average of overlaps between groundtruth and predicted bounding boxes. The success rate measures the percentage of successfully tracked frames where the overlaps are exceed 50%. The Table. IV presents the overall performance of our approach and other 7 state-of-the-art trackers. Our tracker can achieve competitive performance compared to others. Compared to D3S, our approach achieve gains of 0.7% and 2.1% in terms of AO and SR<sub>0.5</sub>, respectively. Our method has a comparable AO score with OceanOn, which obtains the highest AO score.

## VI. CONCLUSION

In this paper, we propose an two-stage tracker which aims to track the target by taking the advantages of detection and segmentation. The performance evaluated on four benchmarks illustrated that our tracker can achieve state-of-the-art results in terms of accuracy and robustness.

TABLE IV

COMPARISON RESULTS ON GOT-10K DATASET WITH PERFORMANCE MEASURES OF AVERAGE OVERLAP (AO) AND SUCCESS RATE (SR). THE  $SR_{0.5}$  DENOTES THE SUCCESS RATES WHERE THE OVERLAPS ARE EXCEED 50%, AND  $SR_{0.75}$  MEASURES THE SUCCESS RATES OVER THE FRAMES WHERE THE OVERLAPS ARE EXCEED 0.75 %.

	SiamMASK	ATOM	DiMP	SiamFc	SiamFCv2	D3S	OceanOn	Ours
AO $\uparrow$	0.514	0.556	0.611	0.348	0.374	0.597	0.611	0.604
$SR_{0.5}$ $\uparrow$	0.587	0.635	0.717	0.353	0.404	0.676	0.721	0.697
$SR_{0.75}$ $\uparrow$	0.366	0.402	0.492	0.098	0.141	0.462	0.473	0.465

## REFERENCES

- [1] D. S. Bolme, J. R. Beveridge, B. A. Draper, and Y. M. Lui, "Visual object tracking using adaptive correlation filters," in *IEEE Conference on Computer Vision and Pattern Recognition*, 2010, pp. 2544–2550.
- [2] J. Valmadre, L. Bertinetto, J. Henriques, A. Vedaldi, and P. H. Torr, "End-to-end representation learning for correlation filter based tracking," in *IEEE Conference on Computer Vision and Pattern Recognition*, 2017, pp. 5000–5008.
- [3] B. Li, J. Yan, W. Wu, Z. Zhu, and X. Hu, "High performance visual tracking with siamese region proposal network," in *IEEE Conference on Computer Vision and Pattern Recognition*, 2018, pp. 8971–8980.
- [4] Z. Zhipeng, H. Peng, J. Fu, B. Li, and W. Hu, "Ocean: Object-aware anchor-free tracking," in *European Conference on Computer Vision*, 2020.
- [5] Q. Wang, L. Zhang, L. Bertinetto, W. Hu, and P. Torr, "Fast online object tracking and segmentation: A unifying approach," in *IEEE Conference on Computer Vision and Pattern Recognition (CVPR)*, 2019.
- [6] A. Lukezic, J. Matas, and M. Kristan, "D3s - a discriminative single shot segmentation tracker." in *IEEE Conference on Computer Vision and Pattern Recognition*, 2020.
- [7] M. Kristan, A. Leonardis *et al.*, "The visual object tracking vot2016 challenge results," in *European Conference on Computer Vision Workshops*, vol. 8926, 2016, pp. 191–217.
- [8] M. Kristan, A. Leonardis, J. Matas *et al.*, "The sixth visual object tracking vot2018 challenge results," in *Proceedings of the European Conference on Computer Vision (ECCV)*, 2018, pp. 0–0.
- [9] M. Kristan, A. Berg, L. Zheng, L. Rout, and L. Zhou, "The seventh visual object tracking vot2019 challenge results," in *2019 IEEE International Conference on Computer Vision Workshop (ICCVW)*, 2019.
- [10] F. Li, C. Tian, W. Zuo, L. Zhang, and M.-H. Yang, "Learning spatial-temporal regularized correlation filters for visual tracking," in *IEEE Conference on Computer Vision and Pattern Recognition*, 2018, pp. 4904–4913.
- [11] A. Lukežič, T. Vojšič, L. Č. Zajc, J. Matas, and M. Kristan, "Discriminative correlation filter with channel and spatial reliability," in *IEEE Conference on Computer Vision and Pattern Recognition*, 2017, pp. 4847–4856.
- [12] M. Danelljan, G. Hager, F. Shahbaz Khan, and M. Felsberg, "Learning spatially regularized correlation filters for visual tracking," in *IEEE International Conference on Computer Vision*, 2015, pp. 4310–4318.
- [13] K. Dai, D. Wang, H. Lu, C. Sun, and J. Li, "Visual tracking via adaptive spatially-regularized correlation filters," in *Proceedings of the IEEE Conference on Computer Vision and Pattern Recognition*, 2019, pp. 4670–4679.
- [14] L. Bertinetto, J. Valmadre, J. F. Henriques, A. Vedaldi, and P. H. Torr, "Fully-convolutional siamese networks for object tracking," in *European Conference on Computer Vision*, 2016, pp. 850–865.
- [15] Z. Zhu, Q. Wang, B. Li, W. Wei, and J. Yan, "Distractor-aware siamese networks for visual object tracking," in *European Conference on Computer Vision*, 2018, pp. 101–117.
- [16] P. H. O. Pinheiro, R. Collobert, and P. Dollár, "Learning to segment object candidates," in *Advances in Neural Information Processing Systems 28: Annual Conference on Neural Information Processing Systems 2015, December 7-12, 2015, Montreal, Quebec, Canada*, 2015, pp. 1990–1998.
- [17] L. Huang, X. Zhao, and K. Huang, "Got-10k: A large high-diversity benchmark for generic object tracking in the wild," *arXiv preprint arXiv:1810.11981*, 2018.
- [18] H. Fan, H. Ling, L. Lin, F. Yang, P. Chu, G. Deng, S. Yu, H. Bai, Y. Xu, and C. Liao, "Lasot: A high-quality benchmark for large-scale single object tracking," in *IEEE Conference on Computer Vision and Pattern Recognition*, 2019, pp. 5374–5383.
- [19] X. Ning, Y. Linjie, F. Yuchen, Y. Dingcheng, L. Yuchen, Y. Jianchao, and H. Thomas, "Youtube-vos: A large-scale video object segmentation benchmark," *arXiv*, 2018.
- [20] M. Danelljan, G. Bhat, F. S. Khan, and M. Felsberg, "Eco: Efficient convolution operators for tracking," in *IEEE Conference on Computer Vision and Pattern Recognition*, 2017, pp. 6931–6939.
- [21] B. Li, W. Wu, Q. Wang, F. Zhang, J. Xing, and J. Yan, "Siamrpn++: Evolution of siamese visual tracking with very deep networks," in *IEEE Conference on Computer Vision and Pattern Recognition*, 2019, pp. 4282–4291.
- [22] Z. Chen, B. Zhong, G. Li, S. Zhang, and R. Ji, "Siamese box adaptive network for visual tracking," in *IEEE Conference on Computer Vision and Pattern Recognition*, 2020.
- [23] M. Danelljan, G. Bhat, F. S. Khan, and M. Felsberg, "Atom: Accurate tracking by overlap maximization," in *IEEE Conference on Computer Vision and Pattern Recognition*, 2019, pp. 4660–4669.
- [24] G. Bhat, M. Danelljan, L. Van Gool, and R. Timofte, "Learning discriminative model prediction for tracking," in *IEEE International Conference on Computer Vision*, 2019, pp. 6182–6191.